THE UNIVERSITY of EDINBURGH

Edinburgh Research Explorer

Experimental study on progressive collapse-resistant behaviour of planar truss

OPEN ACCESS

Experimental study on progressive collapse-resistant behavior of planar trusses

Xianzhong Zhao [a,b], Shen Yan [b], Yiyi Chen [a,b], Zhenyu Xu [b], Yong Lu [c]

a. State Key Laboratory of Disaster Reduction in Civil Engineering, Tongji University, Shanghai, China

b. Department of Structural Engineering, Tongji University, Shanghai, China

c. Institute for Infrastructure and Environment, School of Engineering, University of Edinburgh, Edinburgh, United Kingdom

Abstract:

This paper presents an experimental study on the dynamic progressive collapse behavior of planar trusses. A specially designed member-breaking device has been invented to 'break' a predefined structural member suddenly, particularly a diagonal member in the experiments. Videogrammetric technique was adopted to obtain the full field 3D displacement of the remaining structure, and strain instrumentation was carefully used to monitor the internal forces of all members. In association with the experiments, finite-element simulations of the test trusses have also been performed, with extended analysis on the effect of removal of members at different locations. Experimental results in conjunction with the numerical analysis have shown that: (1) the truss with directly welded joints (specimen truss-WJ) was able to quickly regain balance upon member loss, and the load-redistributing capacity was provided mainly through catenary action developed in the bottom chord; (2) the truss with pinned joints (truss-PJ) behaved almost identically to truss-WJ, suggesting that when computational models of truss structures need to be developed to obtain

structural responses under a collapse scenario, pinned-joints with continuous chord could be

assumed; (3) the truss with rigid joints (truss-RJ) experienced progressive buckling of three

diagonal members and was damaged severely, indicating a detrimental influence of excessive joint

stiffness on the collapse resistance of trusses.

Keywords:

Planar truss, member removal, progressive collapse, collapse-resisting mechanism, joint stiffness

1. Introduction

Building structures may be subjected to man-made (by accident or act of terrorism) or natural hazards, causing local failure such as loss of one or more load-carrying members. As a result, a progressive collapse of the entire structure may be triggered. American Society of Civil Engineers (ASCE) Standard 7 defines progressive collapse as "the spread of an initial local failure from element to element resulting eventually in the collapse of an entire structure or a disproportionately large part of it" [1].

Since the destruction of the Alfred P. Murrah Federal Building in 1995 [2] and the collapse of the World Trade Center towers in 2001 [3], the engineering community, including codes and standards development organizations, public regulatory agencies and research institutions, has been paying significant attention to the performance of buildings subjected to damage from abnormal events. A large number of studies have been conducted, including experimental studies [4-8] and numerical investigations [9-13]. Based on these studies, structural robustness assessment methods have been proposed [14-19], and codes and guidelines for design against progressive collapse of structures have also been released or updated [1, 20-23]. However, up to date, most of the studies have focused on the collapse resistance mechanism of frame structures, whereas relevant information on space structures, especially on large-span roofing systems, is very limited. Space structures can have a number of types and forms, and the load-carrying mechanisms rely heavily on the structural shapes. This is very different from frame structures, and thus the potential collapse resistance mechanism of the space structures can be different from that of the frame structures. The rule of the key members which may be 'removed' due to the accidental load can also be different between normal building frames and space structures. Moreover, space structures

are usually constructed as important public buildings capable of accommodating a large number of people. Collapse of these structures will cause significant casualties and substantial property losses. Hence, the progressive collapse mechanism of space structures is also an important subject, and considering the sparse data currently available, there is an urgent demand for studies on this front.

Truss is one of the most commonly used forms of large-span roofing systems. Available studies on progressive collapse performance of this type of space structures were mainly carried out employing the Alternate Path Method, in which a load-bearing element was instantaneously removed to evaluate the general integrity of a structure and its capacity in redistributing the loads following severe local damage. Studies conducted by Murtha-Smith et al. [24], Malla et al. [25] and Jiang et al. [26] have shown that although truss structures usually have a large degree of redundancy, progressive collapse could occur following the loss of one of the critical members. However, all of the above studies were conducted through finite-element analysis, whereas experimental studies were few. Physical tests are necessary to directly reflect the nonlinear behavior of space structures in collapse scenarios and provide benchmark data for the validation of finite-element models.

In practical engineering applications of tubular trusses or traditional trusses constructed from profile steel members, partially rigid joints (e.g. by welding) are usually adopted. But when a calculation model needs to be developed to obtain the structural response, engineers often assume idealized pinned or rigid joints, as shown in Fig. 1, instead of considering the partial-rigid characteristic of the truss joint because the latter is more computationally expensive. The adequacy of the idealizations for progressive collapse design should also be examined from the

4

structural analysis point of view. In a pinned-joint model, the chords may be treated as discontinuous at joints (see Fig. 1(a)) when there is no external load over the chord members or otherwise continuous (see Fig. 1(b)). However, when analyzing a progressive collapse scenario, the pinned-joint model with a discontinuous chord would not be appropriate in any case because it overlooks the resistance provided by the bending moment in the actual continuous chord and thus underestimates the collapse resistance of the overall structure. An idealization with rigid joints and/or pinned joints with continuous chord may need to be adopted in a progressive collapse analysis of truss structures with welded joints, but the extent to which such modelling idealization may affect the accuracy of the analysis need to be evaluated based on experimental evidences.

This paper presents a comprehensive experimental study on the dynamic progressive collapse resistance of planar trusses, which constitute a basic form of large-span space trusses. Three reduced-size planar Warren trusses have been tested under a sudden loss (removal) of a diagonal member. The three tested trusses had the same geometric and material properties but different types of joints, and they were subjected to identical applied loading conditions. The first truss (referred as specimen truss-WJ) was a typical tubular truss with welded joints. The other two trusses, referred as specimen truss-PJ and truss-RJ, had specially-designed joint connectors which enabled the diagonal members to connect to the continuous chords in perfectly pinned (-PJ) or rigid (-RJ) fashion, respectively. By comparing the three cases, the collapse resisting mechanisms of the practical welded-joint truss can be revealed, and the influence of the joint stiffness on the progressive collapse resistance of a truss structure can also be studied. Furthermore, the experiment and the associated analysis contribute to establishing a library of benchmark models of space structural systems for future numerical and parametric studies.

2. Test program

2.1 Specimens

Three tested trusses were carefully prepared and tested. The first specimen, truss-WJ, was a typical planar Warren truss with directly-welded joints and was designed according to Chinese Code for design of steel structures (GB50017) [27]. As shown in Fig. 2, the truss had a span of 4.0 m and a height of 0.45 m. The top chord (TC), bottom chord (BC) and diagonal members (DM) were constructed using DIN2391 St.35 steel pipes. The cross-sections and mechanical properties are shown in Table 1. The diagonal members were directly welded to the top and bottom chords. The two edge supports (SJ1 and SJ2) were made as fixed pins with full horizontal restraints. It should be noted that in practice the horizontal stiffness provided by the supports may vary depending on specific construction detailing. Using fixed-pin supports without horizontal degree of freedom were adopted to represent an upper bound pinned-support condition for the trusses. Recognizing that different behavior may be observed if the horizontal restraining conditions are changed, this effect may need further studies, but this is not within the scope of this study.

The second and the third specimens, i.e. truss-PJ and truss-RJ, had the same geometric and material properties as those of truss-WJ; but instead of using directly welded joints in truss-WJ, specially designed pinned joint connectors and rigid joint connectors were adopted for Truss-PJ and truss-RJ, respectively, as shown in Fig. 3. The pinned joint connector (see Fig. 3(a)) was comprised of four precisely machined parts:

a: a top steel block whose bottom was machined with a half-cylinder groove with the same diameter as the chord member;

b: a bottom steel block whose top was machined with an identical half-cylinder groove and

bottom was machined with a lug plate;

    c: two steel sleeves with ear plates on top; and

    d: two pins that connected the steel sleeves to the lug plate of bottom steel block.

When truss-PJ was constructed, the chords were clamped by the steel blocks through welding and bolts, and each diagonal member was extended into the steel sleeve with welding at the interface. In this way, each diagonal member was connected to the chord allowing free rotation around the pin, i.e. the in-plane rotational degree of freedom was released. For truss-RJ, the rigid joint connector (see Fig. 3(b)) was similar to the pinned joint connector except that there was no lug plate in the bottom steel block, nor ear plates existed in the steel sleeve; the steel sleeve was directly welded to the bottom surface of the bottom steel block. The welding was sufficiently strong such that no relative translational and rotational movement was allowed between the steel sleeve and the bottom steel block. Meanwhile, in order to apply a point load at each top chord joint (the detailed procedure will be elaborated subsequently), two vertical holes were machined in the steel blocks of each top chord joint connector. For truss-WJ, because it had no joint connectors, one extra top steel block was welded onto the top surface of the top chord at each joint location for carrying the applied point load, as shown in Fig. 3 (c).

Each tested truss was subjected to static loading before the sudden member removal. The amount of the applied static load was determined according to the design roof loads. Truss-WJ was designed as one piece of planar truss unit in a roof system with 1.25 m spacing between adjacent planar truss units. The roof system had a uniformly distributed roof load of 1.59 kPa, including 0.84 kPa dead load and 0.75 kPa live load, thus for truss-WJ, 1.0 kN point load was applied on each edge top chord joint (TJ1 and TJ5), and 2.0 kN point load was applied on each

middle top chord joint (TJ2, TJ3 and TJ4). For truss-PJ and truss-RJ, their self-weights were different from truss-WJ because heavier joint connectors were adopted, hence, slightly reduced joint loads were applied on these two trusses to ensure all the tested trusses were under the same static loading condition. Each point load was applied by means of weights (iron plates) through a pair of hanger rods, which were attached to each top chord joint connector by threading through the holes in the steel blocks.

2.2 Initial damage replication

Progressive collapse of building structures is triggered by local damage which normally occurs suddenly causing dynamic action, therefore, it is preferable to start a dynamic progressive collapse test by suddenly removing a key structural member. For large-span structures such as trusses, there is no codified recommendation on which member to be removed in an Alternate Path Method analysis, and according to the basic concept of the Alternate Path Method, the removed member could be any structural member. In this study, a diagonal member, namely DM2, was chosen as the removed member in all the three tests. This choice was made for the following reasons: a) removing one of the inner diagonal members would create a collapse scenario involving significant rotation at the truss joints due to the creation of an unstable parallelogram grid, thus the influence of joint stiffness could be observed more clearly, and b) under static loading, the internal force in DM2 was found to be the largest among all the inner diagonal members, hence its removal could generate the largest unbalanced force.

Members can be removed in several ways, but in general, a good initial damage replication method should have the following characteristics: a) the method must not change the static behavior of the specimens before the member removal; b) members are removed in a rapid fashion

to well capture the dynamic feature of an instantaneous member loss; c) the method should exhibit consistent performance to facilitate direct comparisons of different tests; d) to make the experimental program a benchmark, the method would be preferred if it generates no extra dynamic impact energy into the remaining structure, in other words, the members being removed should carry no initial kinetic energy.

To satisfy the above requirements, a mechanical member-breaking device was proposed and adopted in this study (Fig. 4). The basic idea of using this device is as follows. Before the test, the middle part of the target member to be removed is deliberately cut, and the gap is then 'repaired' by using the member-breaking device to join the two parts together, thus this member can be considered as 'intact' with this device is in place but is re-broken when the device is taken off. To realize this idea, the member-breaking device was designed to consist of five parts, as shown in Fig. 4(a), namely:

a: two steel cylinders with trapezoid grooving, each welded to one part of the broken member (see Fig. 4(b));

b: a scissors-type clamper; the inner surface of its head was also trapezoid-grooved and thus could interlock with the grooved steel cylinders to join the two parts of the broken member together (see Fig. 4(b));

c: two electromagnets fixed to the tail plates of the scissors-type clamper, to provide the required clamping force at the clamper head through lever action when power is on (see Fig. 4(c));

d: pre-compression springs between the tail plates of the scissors-type clamper, to help accelerate the release-opening of the clamper as soon as the power to the electromagnets is switched off;

e: pre-tension springs attached at one tail plate of the scissors-type clamper (note: only one plate, otherwise the clamper shall not open), and these springs help drag the clamper away immediately after its release so as to ensure a complete disengagement of the member being removed (see Fig. 4(d)).

During the test preparation, the electromagnets were kept powered off to avoid overheating, and a protection clamp was used to install the device on the removed member, as shown in Fig. 4(e).

The applied electromagnet attraction should be large enough to provide a sufficient clamping force at the scissors-type clamper head and thus to ensure complete interlocking between the clamper head and the grooved steel cylinders. The minimum required electromagnet attraction may be calculated as:

$$T = \frac{l}{L} \cdot \left(\frac{2}{\pi} \cdot N \cdot \cot\theta + M \cdot \frac{1}{d} \right)$$ (1)

where, T is the minimum electromagnet attraction required, N and M are the axial force and bending moment of the removed member; l and L are the distance from the axis of rotation to the center of the clamper head and electromagnets, respectively, as shown in Fig. 4(c); θ is the sloped angle of the trapezoid grooving, d is the distance between the center of trapezoid grooving and the center of the un-grooved part, as shown in Fig. 4(b).

2.3 Test setup

Fig. 5 shows the entire test setup. Each tested truss was pin-supported on two reaction frames of which the bases were anchored to a strong floor of the test facility. The height of the reaction frame was 1.6 m, providing sufficient space for large deflection of the tested truss under the collapse scenario. Meanwhile, in order to ensure that the tested truss only deformed in the vertical

plane (which can be true as planar truss was normally braced by purlins in a truss roofing system), a pair of plexiglass plates was placed on both sides of the tested truss; each plexiglass plate was installed on a rectangular frame that was fixed to the top surface of the reaction frames and braced by two triangular frames at both points of trisection. The plexiglass plates were transparent, thus they did not obstruct the experimental observation and the truss displacement measurement by means of the videogrammetric technique, which will be presented later. Vertical plexiglass stiffening ribs were attached on the outer surface of the plexiglass plates to increase their lateral stiffness.

2.4 Instrumentation

During the collapse process of a structure, its geometrical shape usually changes rapidly. Traditional transducers through contact (e.g. linear potentiometers [4], displacement gauges [5, 28], linearity variable differential transducers (LVDTs) [6], and accelerometers [29]) are difficult to be used effectively in such large deformation scenarios [30]. In this study, videogrammetric technique was adopted for a full field measurement of structural dynamic deformation in the 3D domain. Videogrammetric technique uses high-speed cameras at an image rate of at least several hundred frames per second and has been successfully adopted in several existing experimental studies on structural progressive collapse [30-32].

In this study, black rectangular targets with a white circular in the center were adopted as tracking targets and control points. Tracking targets were attached to all truss joints and to the mid-length of all members. Control points were distributed on control network frames which were temporarily constructed around the tested truss, as shown in Fig. 6. Three synchronized high-speed CMOS cameras (Basler ACA 2040-180KM), whose resolution was 2048 pixels ×2048

pixels, were placed in front of the tested truss to capture the image sequences of the tested truss and control network frames. The camera rate was set as 180 frames per second. Through videogrammetric image sequence processing, the tracking targets and control points can be identified and tracked in mass image sequences, and their 3D coordinates in each image can be accurately calculated [26]. In the current laboratory condition with desirable lighting and a clear background, the absolute error of less than 1 mm was achieved.

As the internal force in the structural members also changes rapidly along with the change of structural geometrical shape, full field dynamic strain responses were collected by a strain data acquisition system (DH3820) with a sampling frequency of 100 Hz. The strain measurement locations included mid-length areas of all members, and other potential large bending moment locations according to a preliminary analysis of the response; these included both ends of members TC1~TC2 and BC1~BC2 in all the three trusses, and both ends of W1~W4 in truss-RJ and truss-WJ. At each location, three strain gauges were attached along the direction of the member length, and the three strain gauges were arranged at equal distance around the circumference of the cross-section (i.e. with a 120° angle between lines connecting the strain gauges to the center of the member cross-section). Based on these three strain gauges, the axial force and both in-plane and out-of-plane bending moments could be explicitly calculated.

Meanwhile, in order to double-check whether 100 Hz was high enough to track the high-frequency strain response, the strain of the members around the removed member was additionally collected via another data acquisition device (DH5922) with a high sampling frequency of 10000 Hz.

3. Test results

3.1 Performance of the member-breaking device

The performance of the member-breaking device adopted in this study was evaluated first. As shown in Fig. 7(a), before member removal, the members at symmetric locations of truss-WJ had almost identical axial internal forces (as represented by the averaged strains at the mid-length of members) under the symmetric static load. This confirmed that the insertion of the device effectively maintained the static behavior of the "intact" test trusses. Similar symmetric force distributions were also observed in other two test trusses (not shown here).

Upon triggering the member removal, it took only 0.06 seconds for the internal force of the removed member to totally vanish, as shown in Fig. 7(b). On the other hand, the basic natural vibration periods of truss-PJ and truss-RJ with DM2 removed were analyzed using a finite-element model, and it was found that these periods were 0.95 s and 0.61 s, respectively. For truss-WJ, because the stiffness of joints was between that in truss-PJ and truss-RJ, the basic natural vibration period with DM2 removed should be between 0.95s and 0.61s. The general guideline [20] requires that in a dynamic progressive collapse analysis of frame structures the member removal should be within a time period that is no more than 1/10 of the period associated with the structural response mode after the element removal. Therefore, the member-removal processes in all three tests were sufficiently rapid.

Furthermore, the axial force reduction condition of the removed member DM2 (based on averaged strains) in all three tests followed almost the same trend, indicating that this device had stable and consistent performance in removing members. No evident fluctuations occurred in the strain curves of DM2 when the baseline was reduced to zero, indicating that there was no

unwanted extra kinetic energy input into the remaining structure. To summarize, the member-breaking device was effective and exhibited a reliable and consistent performance for dynamic progressive collapse tests.

3.2 Strain data acquisition and sampling frequencies

Fig. 8 presents the strain responses collected by strain gauge A, which was the strain gauge installed on the top surface of a member, for members DM3 and TC1 in truss-WJ. Two sets of the time history curves are included, using two different sampling frequencies of 100 Hz and 10000 Hz, respectively. The internal forces of these two members had high frequency dynamic effects because they were located adjacent to the removed member DM2, and such effect was picked up in the strain data sampled at 10000 Hz. However, the high frequency fluctuation was apparently caused by the member self-vibration and had relatively small amplitude. As far as the main dynamic strain responses are concerned, it can be concluded that a sampling frequency of 100 Hz was sufficient for this experimental program. Therefore, all the strain data presented in the following discussions are based on the sampling frequency of 100 Hz unless stated otherwise.

3.3 Truss-WJ

Upon the removal of DM2, truss-WJ started to deform immediately. Taking the time when the removal of DM2 started as time zero (the discussions for the other tests also followed this definition), the remaining structure regained balance at about 0.46 s. As shown in Fig. 9, the initial local damage did not spread and was limited within the parallelogram grid enclosing DM2. The largest vertical displacement, about 265 mm, was found at BJ1 (refer to Fig. 2 for the locations).

Generally speaking, the removal of a key member would cause a significant disruption of the equilibrium of forces at both local and global levels. Locally, unbalanced forces are generated at

the joints at both ends of the removed member; the process of achieving a new equilibrium of forces at these joints is defined as "Local Internal Force Redistribution" in this paper. Globally, the force flow of the overall structure has to be re-established to bridge over the initial local damage to transfer the external loads to the supports with the altered the load-transfer path of the structure; this process is defined as "Global Internal Force Redistribution" in this paper. For any structure subjected to an initial local member failure, these two types of internal force redistribution have to be well accommodated by the remaining structure, otherwise progressive collapse will occur. It should be noted that if rebalance is eventually achieved then equilibrium must be achieved at both local and global levels; nevertheless, introducing the above "local" and "global" internal force redistribution definitions facilitates better description of the transient processes following the member removal.

For truss-WJ, local internal force redistribution took place at TJ1 and BJ1 after the removal of DM2, as shown in Fig. 9. Taking TJ1 for example, before DM2 was removed, the applied point load at TJ1 was carried by the vertical components of the resultant force of the compressive force in DM1 and the tensile force in DM2. The balanced state was disrupted as soon as DM2 was removed. At this moment, the original vertical component of the compressive force in DM1 was too large for the applied load at TJ1 to balance. Hence, to regain force equilibrium at TJ1, the compressive force in DM1 decreased quickly along with the disappearance of the tensile force in DM2, as shown in Fig. 10. Therefore, the local internal force redistribution mechanism in this truss was realized through self-adjustment of the internal forces in the adjacent members to regain local force equilibrium at the immediately affected joints.

The global internal force redistribution in this truss was a relatively more complex process.

The vertical components of the internal forces in the diagonal members provided vertical resistance for the external load to be transferred to the supports. Hence, after DM2 was removed, there was no vertical resistance at the location where DM2 was originally located. An alternative path was provided to help transfer the external load at joints TJ2 to TJ5 to the left support SJ1, a mechanism corresponding to a global internal force redistribution (see Fig. 9). This process could be subdivided into four stages as shown in Fig. 11, in which, "+" and "-" in the legend represents strain on the top and bottom surface of a member, respectively, which were calculated by three strain gauges through the Plane Section Remains Plane Assumption. Stage I began when the vertical load transfer path at DM2 was completely interrupted at 0.06 s. Because there was no obvious deformation yet at this moment, the vertical load resistance was provided by the shear forces in horizontal chords TC1 and BC1, and bending moment also developed in both members. However, after 0.12 s (Stage II: 0.12 s to 0.31 s), BJ1 moved downwards rapidly along with the ongoing deformation of the remaining structure, and concurrently BC1 was tilted and elongated. Tension action started to dominate in BC1, and in the subsequent response the vertical component of such tension action provided the vertical load resistance. This is the well-known "Catenary Action" mechanism. In the present case with truss-WJ, the resistance offered by the catenary action was determined not only by the tensile force but also by the tilting angle, as expressed by Eq. 2.

$$V_{\text{catenary}} = T_{\text{v}} = T \cdot \sin \alpha \tag{2}$$

where V_{catenary} is the vertical load resistance provided by catenary action; T and T_{v} are tensile force in a tensile member and its vertical component, respectively; α is the tilting angle of the tensile member.

Therefore, despite that the tensile force in BC1 had reached its maximum value of about 18.45 kN (1500 με in tubular section ∅20×1) at 0.18 s, its vertical component was still relatively small because the tilting angle of BC1 was only about 8º (the vertical displacement of BJ1 was 120 mm) at this moment. The shear force in TC1 had to maintain its contribution in providing the vertical load-carrying resistance and thus the value stayed almost constant during this step.

Stage III began at about 0.31s when the tilting angle of BC1 reached 16.7º (the vertical displacement of BJ1 was 234 mm). The vertical load resistance provided by the catenary action became significant enough, allowing the shear force in TC1 to decrease and finally vanished at 0.46 s. At this moment (the beginning of Stage IV), tensile force in BC1 was about 10.09 kN (820 με), and its vertical component was about 3.34 kN with a tilting angle as large as 19º. This force value was quite close to half of the total applied point loads at TJ2 to TJ5 (total load was 7.0 kN), indicating that the axial force in BC1 alone provided an alternative path for the external load to be transferred to the left support. The catenary action became stabilized from then onwards, and the remaining structure regained balance.

Under this balanced configuration, the sub-structure on the right-hand side of DM2 remained undamaged, as shown in Fig. 9. This sub-structure still behaved as a typical Warren truss, where the top chord (TC4) was under compression, the bottom chord (BC4 and BC5) was under tension, and axial force with opposite signs existed in adjacent diagonal members (DM8 and DM9), as shown in Fig. 12 (a). Furthermore, increased tensile force was observed in all the bottom chord members with a similar trend, as shown in Fig. 12(b), and this indicates that the catenary action is a global mechanism and requires the participation of the whole bottom chord. Fig. 12(b) also shows that among all the bottom chord members, the tensile strain in BC3 was evidently larger

than in the other members and exceeded the effective measuring range of the strain gauge used (about 20,000 με). This is because that in a typical Warren truss, such as the sub-structure on the right-hand side of DM2 as discussed above, the largest tensile force exists in the middle bottom chord. Therefore, BC3, which was the middle bottom chord member of the undamaged sub-structure, could be regarded as the "key element" in developing the catenary action and in turn preventing the remaining structure from progressive collapse; if failure occurred in this critical member, the catenary action that help develop the formation of the alternative path will not be formed.

3.4 Truss-PJ

After the removal of DM2, the remaining structure of truss-PJ survived with a re-balanced state at about 0.44 s. As shown in Fig. 13(a), the balanced configuration was very similar to that of truss-WJ. In addition, these two tested trusses shared a similar collapse-resistance mechanism: the compressive force in DM1 reduced to accommodate a local force equilibrium at TJ1 (Fig. 13(b)); the shear force in TC1 and BC1 first helped transfer the external load at TJ2~TJ5 to the left support, and then catenary action developed over the bottom chord (Fig. 13(c)-(d)); BC3 was also the key element in preventing the remaining structure from progressive collapse, where the tensile force in this member was significantly larger than the others. Other load redistribution mechanisms, which were found to be similar to those of truss-WJ, were not repeated here.

3.5 Truss-RJ

Truss-RJ was found to behave differently from the other two specimens. After DM2 was removed, the remaining structure started to deform downwards. At 0.41 s, the diagonal member DM3 buckled suddenly, followed by the buckling of DM5 and DM4 at 0.67 s and 0.87 s,

respectively. The top chord joint TJ2, which was originally supported by DM3 and DM4, started to fall rapidly after both of these two diagonal members buckled and then hit the bottom chord BC2 at 1.17 s. After that, the remaining structure became stabilized thanks to the catenary action, which was developed along the bottom chord similar to the cases of truss-WJ and truss-PJ. However, the entire left part of truss-RJ was damaged severely due to successive failure of three diagonal members (Fig. 14).

Because of the successive buckling of the three diagonal members, both local and global internal force redistributions were interrupted, as shown in Fig. 15. For the process of local internal force redistribution, as soon as DM2 was removed, the compressive force in DM1 decreased towards achieving a force equilibrium at TJ1, a mechanism which was the same as truss-WJ. However, this process was terminated by the buckling of DM3, and DM1 was bended due to the subsequent downward movement of TJ2. Meanwhile, the buckling of the diagonal members generated unbalanced forces at TJ2 and TJ3 as well, and as a result local internal force redistribution had to be achieved at more joints. For example, the compressive force in DM6 increased as soon as DM5 buckled to provide vertical load resistance for TJ3 (see Fig. 15).

With regard to the process of global internal force redistribution in truss-RJ, at the beginning, the combined action of shear force in TC1 and the catenary action in BC1 tended to provide an alternate path for the external load at TJ2~TJ5 to be transferred to the left support SJ1, a mechanism which was the same as truss-WJ. But the buckling of DM3 and the other two diagonal members caused transient unloading of the tensile force in the bottom chord, hence catenary action had not been stabilized in the next 0.5s. In this circumstance, the shear force in TC1 had to keep its contribution in providing the vertical load resistance; the temporary unloading at around

0.7 s was due to the rapid downward movement of TJ2. The catenary action developed in the bottom chord was finally stabilized after TJ2 dropped onto the bottom chord, and as a result the remaining structure was prevented from further deformation.

Across the three tested trusses, on the surface there appeared to be no complete whole-structure collapse occurring. However, comparing to truss-WJ and truss-PJ which regained a balanced state with all the remaining members generally stayed intact, truss-RJ underwent sequential failure in several other diagonal members, leading to severe distortion – effectively partial collapse in the entire left half – of the structure. Therefore it is reasonable to conclude that truss-RJ actually reached a progressive collapse state.

4. Influence of joint stiffness and discussion

4.1 Detrimental influence of excessive joint stiffness

Since different responses were observed for the tested trusses with identical geometry properties and external loading condition, it is reasonable to postulate that the joint stiffness has important influence on the collapse resistance of planar trusses. The balanced configurations of the remaining structures of all the three tested trusses are shown in Fig. 16, which were obtained by 3D laser scanner. Among the three specimens, truss-RJ with the highest joint stiffness was the only one that experienced collapse, as discussed above. This observation appears to contradict the general understanding that stronger and stiffer joints are beneficial for redundancy and thus for the collapse resistance.

To investigate this phenomenon, a comparison of the strain response in DM1, TC1 and BC1 in the three tests is presented in Fig. 17. These members have been demonstrated to be the most important ones in achieving local and global internal force redistributions. It can be noticed that

the members in different tested trusses behaved similarly before 0.41 s, at which moment buckling of DM3 occurred in truss-RJ, indicating that the mechanisms of the local and global internal force redistributions and the associated deformation modes in all the three trusses were similar by that stage. Clearly, the significant difference in the subsequent behavior between truss-RJ and the other tested trusses was primarily attributable to the buckling of DM3 at 0.41 s.

Fig. 18 shows the strain responses in DM3 for the three trusses. The compressive force in DM3 of truss-WJ was no larger than that in the other tested trusses by the time of 0.41 s. However, the bending moment at the member end of DM3 was totally different. In truss-PJ, there was no bending moment at the diagonal member ends. In truss-WJ where the joints were partially rigid, the bending strain was about 1400 $\mu\varepsilon$. In contrast, in truss-RJ with perfectly rigid joints, the bending strain was up to 5600 $\mu\varepsilon$. Such a large bending moment reduced the buckling strength of DM3 considerably and caused its buckling to occur, and this in turn resulted in the progressive collapse of the whole structure. From this point of view, the diagonal member adjacent to the removed member DM2, in this case DM3, should also be regarded as a "key element" whose failure might cause the severe damage to the remaining structure.

A further explanation on why large bending moment occurred at the ends of the diagonal members in the truss with rigid joints, when subjected to the sudden loss of a diagonal member, is given herein. As schematically demonstrated in Fig. 19, after a diagonal member AD was removed, the parallelogram grid ABCD was bound to distort because the bottom chord CD was elongated due to the catenary action developed to provide the alternate load-transferring path. Hence, bending moment was generated at both ends of the diagonal member BD in truss-RJ with rigid joints, whereas the bending moment was released in truss-PJ with pinned joints.

Considering that the catenary action usually leads to significant deformation of the overall structure and thus the distortion of the truss grids, it may be reasonable to postulate that in terms of the progressive collapse resistance the joints of a truss need not be made too stiff or rigid. Otherwise, significant bending moment could develop at the ends of the diagonal members, leading to early buckling and consequently the progressive collapse of the whole truss structure.

From the test of truss-WJ, marked rotation at joint BJ1 was observed, and the angle between members DM2 and DM3 was reduced by 15°. This indicated that the stiffness of the directly welded tubular joint was less significant under the collapse scenario. As such, the catenary action developed well in this truss and no local buckling occurred, and this helped avoid the progressive collapse.

At this juncture, it is worth noting that in practical engineering applications joint strengthening measures such as stiffening plates and chord enhancement are sometimes adopted to increase the strength of a joint. The current finding raises a question that these measures may compromise the rotational capacity of the joint and thus may in turn reduce the collapse resistance of the whole structure.

4.2 On the assumption of joints in simplified truss analysis model

As previously discussed in Section 1, when a calculation model needs to be developed to obtain the progressive collapse resistance of a truss with welded joints, the joints may be assumed as idealized rigid joints or idealized pinned joints with a continuous chord. Both assumptions may be regarded as suitable under normal loading conditions. However, according to the performance comparison between truss-RJ and truss-WJ discussed above, in a collapse scenario the diagonal members in a rigid-joint model could end up with easier buckling than that in the actual

welded-joint truss. Hence, the two assumptions mentioned above could yield very different collapse resistance predictions.

For truss-PJ (a pinned-joint truss with continuous chord), it exhibited the same collapse-resistance mechanism and a very similar balanced configuration (see Fig. 16) as compared with truss-WJ (a welded-joint truss). The strain responses in the most critical members, including the members that were responsible for the local and global internal force redistribution (DM1, TC1 and BC1, see Fig. 17) and DM3 that tended to buckle first to cause structural collapse (see Fig. 18), were also very close between these two trusses. It should be noted that for the strain in BC3 which was also regarded as a key element in developing the catenary action, its peak value in truss-WJ exceeded the measuring range of the strain gauges (20,000$\mu\epsilon$ herein), while in truss-PJ its peak value was just about 12,500$\mu\epsilon$ (see Fig. 12(b) and Fig. 13(d)). Although these absolute strains were quite different, they were both in advanced yield regions; moreover the difference of the tensile forces within BC3 in these two tested trusses was very limited as both magnitudes of the strains were in the hardening stage of the mild steel material. Based on the force equilibrium calculations at BJ2, the difference of the tensile force was only 3%. The above results tend to suggest that a pinned-joint model in conjunction with a continuous chord could reasonably represent the primary response of a welded-joint truss in the analysis of a progressive collapse scenario, thus simplifying the modelling effort for a welded-joint truss considerably. Of course the extent to which such a simplification approach may be applied for different types of truss structures would require further study.

5. Finite-element investigations

5.1 FE modelling considerations

Finite element analysis has been conducted to assist in the interpretation of the experimental results and perform further numerical investigations. For the purpose of the present paper, the FE analysis of truss-PJ and truss-RJ, which need not involve very detailed continuum FE model, is described in this section.

These FE models are developed in commercial FE package ABAQUS [33]. The truss members are modeled with two-node linear space beam elements (element type "B31") with pipe cross-section, and the material is modeled using a piecewise-linear plasticity model with stress-strain curves based on the coupon test data for the experimental truss structures. The joint connectors are modeled with B31 elements with a rectangular cross-section or a circular cross-section, where elastic material model is adopted. The connecting methods between the diagonal members and joint connectors are different for two models. All degrees of freedom are constrained in the truss-RJ model, while the in-plane rotational degree of freedom is released in the truss-PJ model. The point loads are modeled with lumped masses. In order to be consistent with the experiment, the out-of-plane translational and rotational degrees of freedom are fully restrained at all the joints. Moreover, hard contacts between the joint connectors and the opposite chord members are specified to prevent the joint connectors from passing through the chord members.

For the analysis of each test, an implicit time integration (ABAQUS/Standard) analysis is performed first to obtain the static initial condition of the intact truss. The deformed mesh of the truss model and its associated material state is then imported into the explicit time integration

solver ABAQUS/Explicit. To simulate the removal of member DM2, the truss model is modified

with DM2 removed from the mesh but its original internal forces retained. The internal forces are

then deactivated within 0.06 s, following the force reduction curves measured from the experiment

as shown in Fig. 7, to start the dynamic progressive collapse analysis.

5.2 Model validation and comparative results

After the removal of DM2, the FE model of truss-PJ regains a balance with notable vertical

deflection. Comparisons between the FE results and the experimental measurements of several

important structural responses relating to the catenary action development, including the vertical

displacement of BJ1 and the strain responses in BC1, are presented in Fig. 20. Good agreement is

observed between the FE and the experimental results, indicating that the FE model is sufficiently

accurate in representing the dynamic response and the collapse-resisting mechanism of the tested

truss.

The FE model of truss-RJ experiences successive buckling of diagonal members, which is

identical to the experimental observation. As shown in Fig. 21, both the sequence of diagonal

member buckling and the final shape of the remaining structure are well predicted by the FE

analysis. This again confirms that FE analysis can provide an effective way for progressive

collapse study of truss structures and the model can be applied in extended numerical studies.

5.3 Structural responses under different member-loss scenarios

Having verified the FE models and the analysis procedures, in this section we examine the

influence of varying member removal scenarios, as well as the influence of the joint stiffness.

The FE model of truss-PJ is adopted as the reference case to represent both pinned and

welded joint cases. Fig. 22a shows the deformed structure following a sudden removal of another

diagonal member, herein DM5. Similarly to the tests of truss-PJ and truss-WJ, the remaining structure regains a balance through the catenary action developed along the bottom chord, which is characterized by a remarkable overall deflection and large tensile strain in the bottom chord. When initial local failure occurs at a top chord member such as TC2, as shown in Fig. 22b, the catenary action developed along the bottom chord again helps the remaining structure achieve a re-balance state. Therefore, an intact bottom chord is crucial in resisting progressive collapse of trusses. This can also be demonstrated by removing one of the bottom chord members. As shown in Fig. 22c, truss-PJ collapses after a sudden failure of BC1 as no catenary action can be developed in the incomplete bottom chord.

When subjected to the same local failure as in truss-PJ, the truss with rigid joints (truss-RJ) performs differently for most scenarios. Excessive joint stiffness limits the deformability at the joints, as previously discussed, such that the buckling of nearby diagonal members is observed following the sudden removal of a diagonal member or a top chord member, as shown in Fig. 23a and 23b. The above result provides further evidence suggesting the potential detrimental influence of excessive joint stiffness on the collapse resistance of trusses. When the local failure occurs at the bottom chord member, the remaining structure performs similarly to truss-PJ, as shown in Fig. 23c.

6. Conclusions

This paper presented an experimental study on the dynamic progressive collapse of trusses. A dynamic testing apparatus for the progressive collapse test of truss structures was developed, and three planar trusses were tested. One diagonal member in each tested truss was suddenly removed by a member-breaking device, which was invented to break a predefined structural member

suddenly. Videogrammetric technique and strain instrumentation were employed to monitor the global and local deformations of the remaining structure and the redistribution of internal forces. In conjunction with the experiment, finite-element simulations of the tests were also performed to assist in the interpretation and confirmation of the experimental observations. The following main conclusions may be drawn:

(1) The member-breaking device proved to work effectively in simulating a sudden loss of a load-carrying member in a progressive collapse test scenario. The design of the device may be extended to the experiment of other types of structures.

(2) To assist in the analysis of the processes involved in the progressive collapse resistance mechanisms, the concept of local and global internal force redistributions in the remaining structure was put forward, where the former refers to the process of achieving a new force equilibrium state at joints at both ends of the removed member, and the latter refers to the process of redistributing the force flow of the remaining structure to provide alternate path for the external loads to be transferred to the supports.

(3) The truss with directly welded joints (truss-WJ) was capable of regaining a balanced state very quickly (in less than 0.5s herein) after the removal of the designated diagonal member (DM2). The initial local member failure did not spread, and was confined within the parallelogram grid that enclosed the failed member. With the afore-mentioned local and global force redistribution concept, it was found that for truss-WJ, the local internal force redistribution was achieved through re-adapting the internal forces among the members which shared the same joint as the failed member, while the global internal force redistribution was completed mainly through the catenary action developed along the bottom chord.

(4) Truss-PJ (with pinned joints) behaved almost identically to truss-WJ. This observation is also significant in terms of modelling typical welded-joint truss structures, so that the welded joints may be simplified into pinned-joints in conjunction with the assumption of a continuous chord for the progressive collapse analysis of this type of trusses.

(5) For the truss with rigid joints (truss-RJ), however, successive buckling of adjacent diagonal members occurred after the removal of DM2. The buckling of these members significantly weakened the structural capacity of redistributing loads, leading to severe damage of the entire left part of the remaining structure. The tested truss did not totally collapse thanks to the catenary action developed in the bottom chord; however the large deformation state indicated that a progressive collapse had effectively occurred. Such behavior in the rigid-jointed truss tends to suggest that employing very stiff or rigid joints in a truss could adversely affect the structural resistance against progressive collapse.

(6) The above experimental observations are generally confirmed by the finite element analysis. The FE model and the numerical analysis scheme can be applied in extended numerical study of progressive collapse of truss structures of different configurations.

Acknowledgement

program is appreciated.

References

[1] American Society of Civil Engineers (ASCE). Minimum Design Loads for Buildings and Other Structures. Reston, VA: American Society of Civil Engineers; 2010.

[2] Federal Emergency Management Agency (FEMA). The Oklahoma City bombing: Improving building performance through multi-hazard mitigation. FEMA Rep. 277, Washington, DC; 1996

[3] National Institute of Standards and Technology (NIST). The collapse of the World Trade Center towers. NIST NCSTAR 1, Gaithersburg, MD; 2005.

[4] Sasani M, Sagiroglu S. Progressive collapse resistance of Hotel San Diego. Journal of Structural. Engineering ASCE 2008; 134(3): 478-488.

[5] Chen J, Huang X, Ma R, He M. Experimental study on the progressive collapse resistance of a two-story steel moment frame. Journal of Performance of Constructed Facilities 2011; 26(5): 567-575.

[6] Guo L, Gao S, Fu F, Wang Y. Experimental study and numerical analysis of progressive collapse resistance of composite frames. Journal of Constructional Steel Research 2013; 89(0): 236-251.

[7] Song BI, Giriunas KA, Sezen H. Progressive collapse testing and analysis of a steel frame building. Journal of Constructional Steel Research 2014; 94: 76-83.

[8] Wang W, Fang C, Qin X, Chen YY, Li L. Performance of practical beam-to-SHS column connections against progressive collapse. Engineering Structures; 106: 332-347, 2016.

[9] Luccioni BM, Ambrosini RD, Danesi RF. Analysis of building collapse under blast loads. Engineering Structures 2004; 26(1): 63-71.

[10] Kim J, Kim T. Assessment of progressive collapse-resisting capacity of steel moment frames. Journal of Constructional Steel Research 2009; 65(1): 169-179.

[11] Khandelwal K, El-Tawil S, Sadek F. Progressive collapse analysis of seismically designed steel braced frames. Journal of Constructional Steel Research 2009; 65(3): 699-708.

[12] Fu F. Progressive collapse analysis of high-rise building with 3-D finite element modeling method. Journal of Constructional Steel Research 2009; 65(6): 1269-1278.

[13] Fang C, Izzuddin BA, Elghazouli AY, Nethercot DA. Robustness of steel-composite building structures subject to localised fire. Fire Safety Journal 2011; 46(6): 348-363.

[14] Marjanishvili S. Progressive analysis procedure for progressive collapse. Journal of Performance of Constructed Facilities 2004; 18(2): 79-85.

[15] Dusenberry DO, Hamburger RO. Practical means for energy-based analyses of disproportionate collapse potential. Journal of Performance of Constructed Facilities 2006; 20(4): 336-348.

[16] Izzuddin BA, Vlassis AG, Elghazouli AY, Nethercot DA. Progressive collapse of multi-storey buildings due to sudden column loss - Part I: Simplified assessment framework. Engineering Structures 2008; 30(5): 1308-1318.

[17] Lee CH, Kim S, Han KH, Lee K. Simplified nonlinear progressive collapse analysis of welded steel moment frames. Journal of Constructional Steel Research 2009; 65(5): 1130-1137.

[18] Fang C, Izzuddin BA, Elghazouli AY, Nethercot DA. Simplified energy-based robustness

assessment for steel-composite car parks under vehicle fire. Engineering Structures 2013; 49: 719-732.

[19] Fang C, Izzuddin BA, Elghazouli AY, Nethercot DA. Robustness of multi-storey car parks under localised fire - towards practical design recommendations. Journal of Constructional Steel Research 2013; 90: 193-208.

[20] General Services Administration (GSA). Progressive Collapse Analysis and Design Guidelines for New Federal Office Buildings and Major Modernization Projects. Washington, DC: General Services Administration; 2003.

[21] Department of Defense (DOD). Design of buildings to resist progressive collapse. Unified Facilities Criteria (UFC) 4-023-03. Washington, DC: Department of Defense; 2009.

[22] China Association for Engineering Construction Standardization (CECS). Code for anti-collapse design of building structures. CECS 392-2014. Beijing: China Planning Press; 2015.

[23] Japanese Society of Steel Construction & Council on Tall Buildings and Urban Habitat. Guidelines for Collapse Control Design - Construction of Steel Buildings with High Redundacy, Vol. 1 Design. Tokyo, Japan Iron and Steel Federation (JISF); 2005.

[24] Murtha-Smith E. Alternate path analysis of space trusses for progressive collapse. Journal of Structural Engineering ASCE 1988; 114(9): 1978-1999.

[25] Malla RB, Nalluri BB. Dynamic nonlinear member failure propagation in truss structures. Structural Engineering and Mechanics 2000; 9(2): 111-126.

[26] Jiang X, Chen Y. Progressive Collapse Analysis and Safety Assessment Method for Steel Truss Roof. Journal Performance of Constructed Facilities 2012; 26(3): 230-240.

[27] Ministry of Construction of the People's Republic of China. Code for design of steel structures. GB 50017-2003. Beijing: China Planning Press; 2003.

[28] Rodriguez-Nik TR, Lee CS, Hegemier GA, Seible F. Experimental performance of concrete columns with composite jackets under blast loading. Journal of Structural Engineering ASCE 2012; 138(1): 81–89.

[29] Wu CL, Kuo WW, Yang YS, Hwang SJ, Elwood KJ, Loh CH, et al. Collapse of a nonductile concrete frame: shaking table tests. Earthquake Engineering and Structural Dynamics 2009; 38 (2): 205–224.

[30] Liu X, Tong X, Yin X, Gu X, Ye Z. Videogrammetric technique for three-dimensional structural progressive collapse measurement. Measurement 2015; 63: 87-99.

[31] Li Y, Lin F, Gu X, Lu X. Numerical research of a super-large cooling tower subjected to accidental loads. Nuclear Engineering and Design 2014; 269: 184-192.

[32] Chen Y, Wang L, Yan S, Zhao X. Study on the progressive collapse of large span truss-beam structures induced by initial member break. Safety, Robustness and Condition Assessment of Structures 2015; 112-119.

[33] ABAQUS Inc. ABAQUS Release 6.10 Documentation. RI: ABAQUS Inc., 2010.

Table 1. Cross-sections and mechanical propeties of members

	Cross-section	Yield strength	Ultimate strength	Fracture strain
TC	$\phi 25 \times 1.5$	300	409	0.26
BC	$\phi 20 \times 1$	305	418	0.26
DM	$\phi 14 \times 1$	278	415	0.35

[a] Fracture strain is based on proportional coupon gauge length of $5.65\sqrt{S_0}$, where S_0 = orginal cross-section area of coupons.

(a)   (b)   (c)
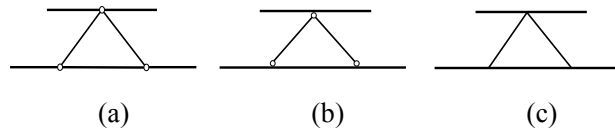
Fig. 1. Simplified joint assumption in truss model. (a) pinned joint with discontinuous chord; (b) pinned joint with continuous chord; (c) rigid joint
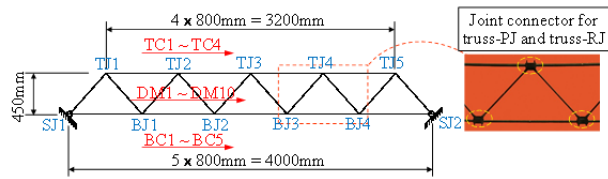
Fig. 2 Overview of the tested trusses

(a)

(b)

(c)
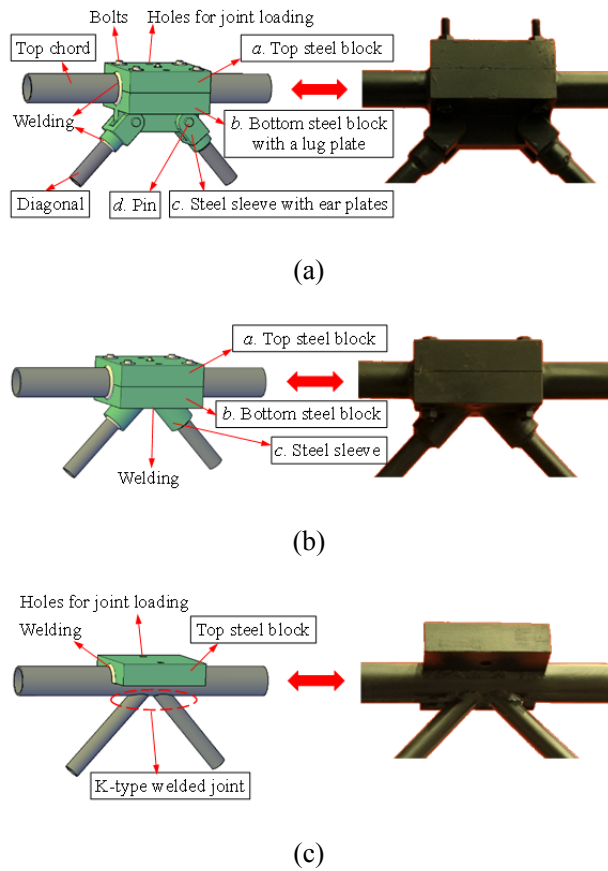
Fig. 3. Joint construction details. (a) pinned joint connector in truss-PJ; (b) rigid joint connector in truss-RJ; (C) welded joint and attached steel block in truss-WJ

(a)

(b)

(c)

(d)

(e)
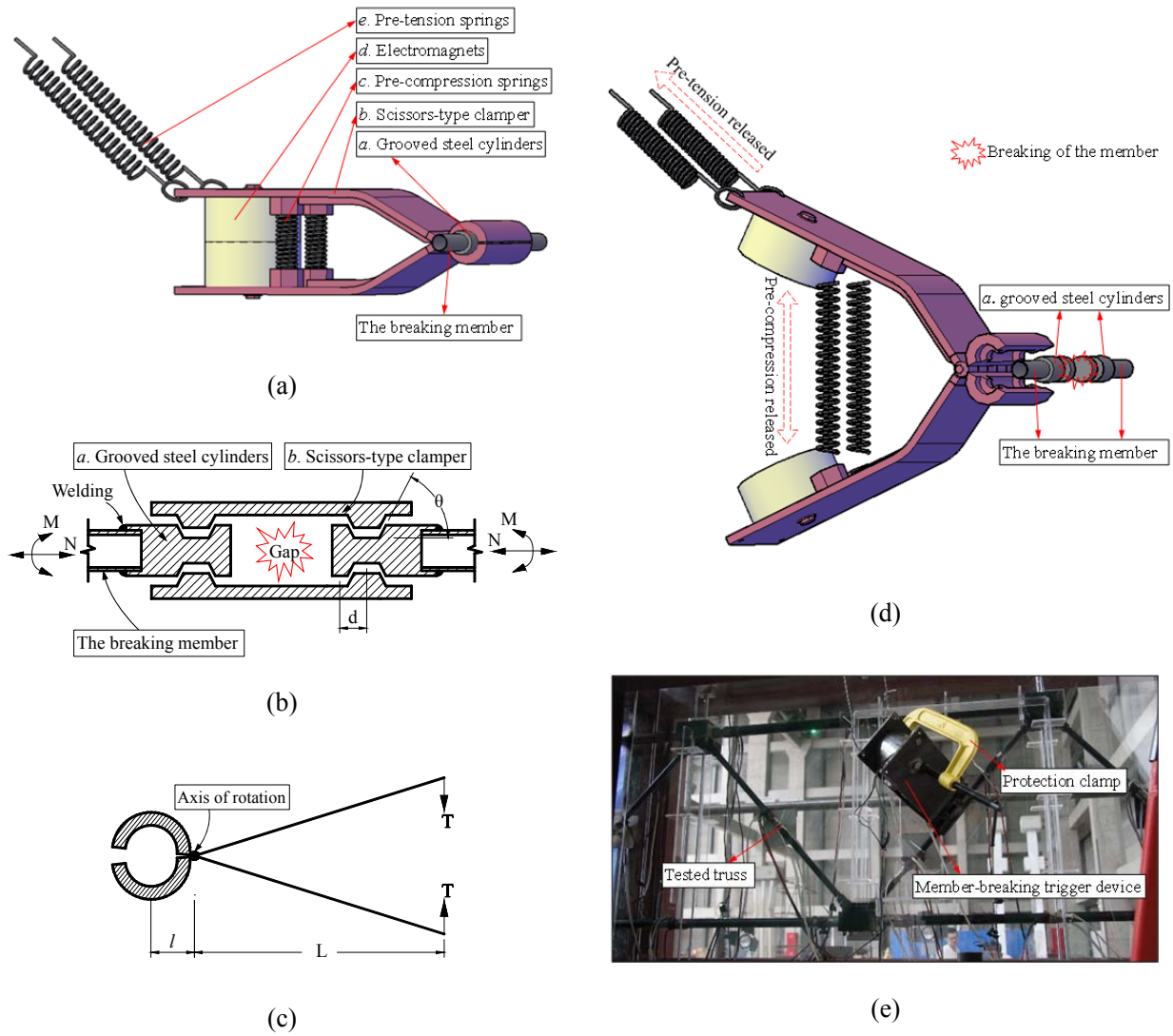
Fig. 4. Illustration of the member-breaking device and its various components

(a)

(b)
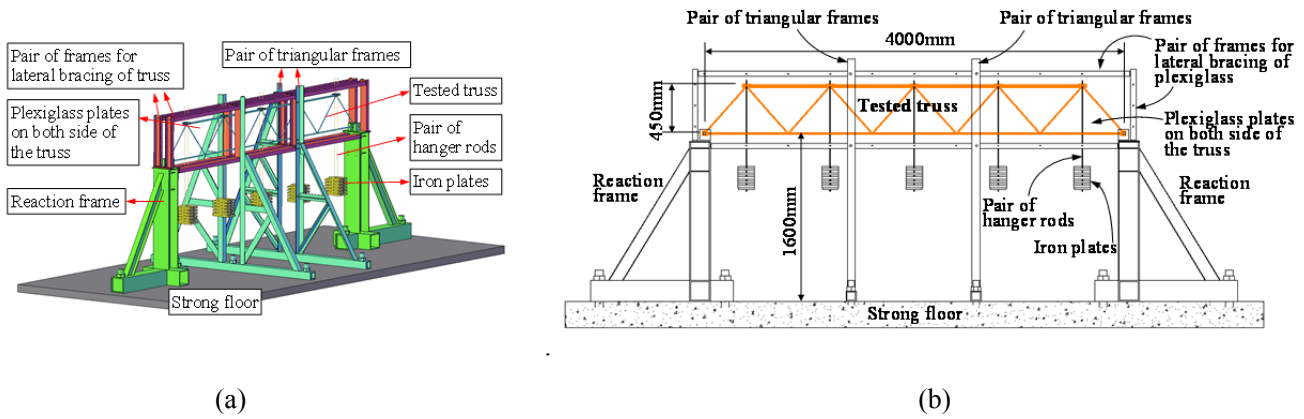
Fig. 5 Test setup. (a) aerial view; (b) elevation view
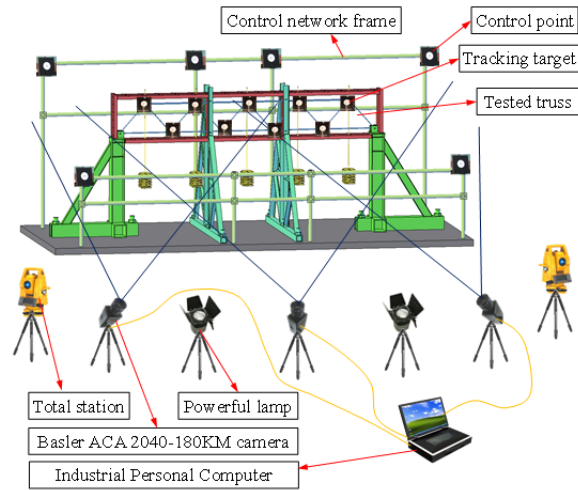
Fig. 6 High-speed videogrammetric measurement system.

(a)

(b)
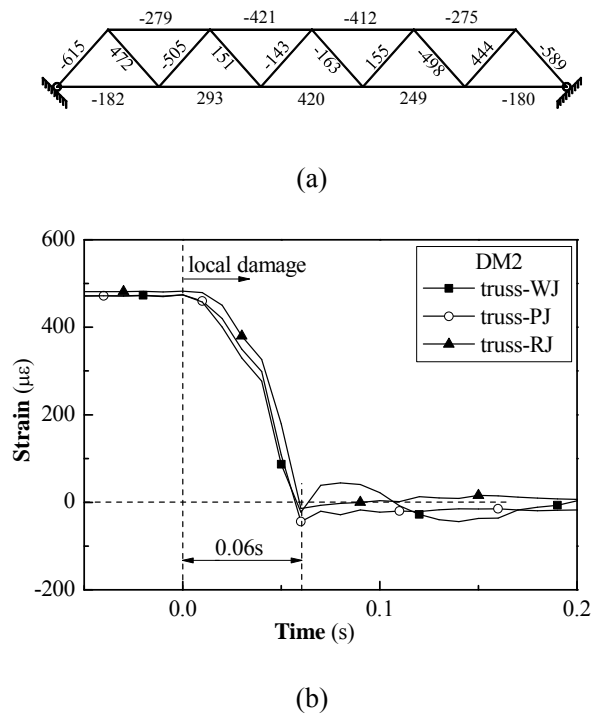
Fig. 7. Performance of the member-breaking device. (a) averaged strains at the mid-length of all members in truss-WJ when statically loaded; (b) averaged strains in DM2 of all three test trusses.
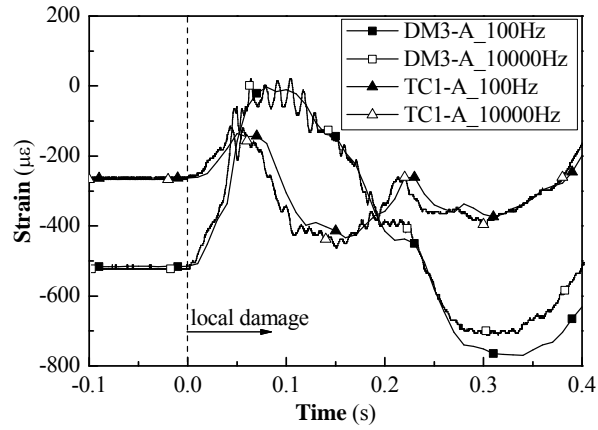
Fig. 8. Strain responses in truss-WJ collected with different sampling frequencies.
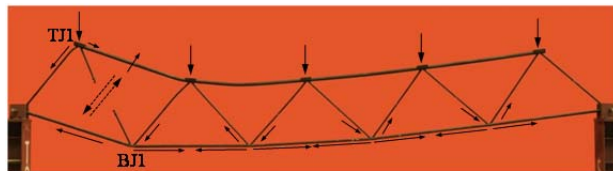
Fig. 9. Balanced configuration and the force flow of truss-WJ
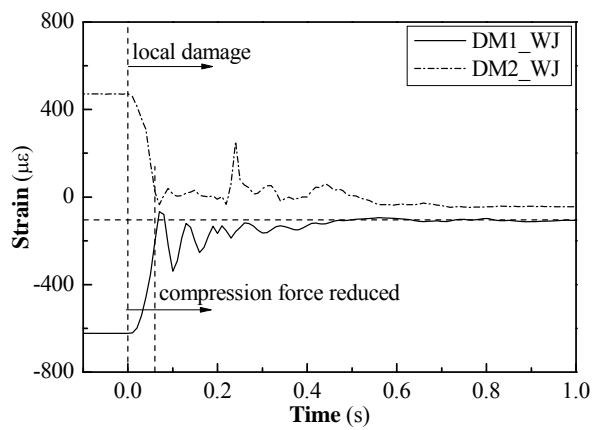
Fig. 10 Local internal force redistribution at joint TJ1 in truss-WJ
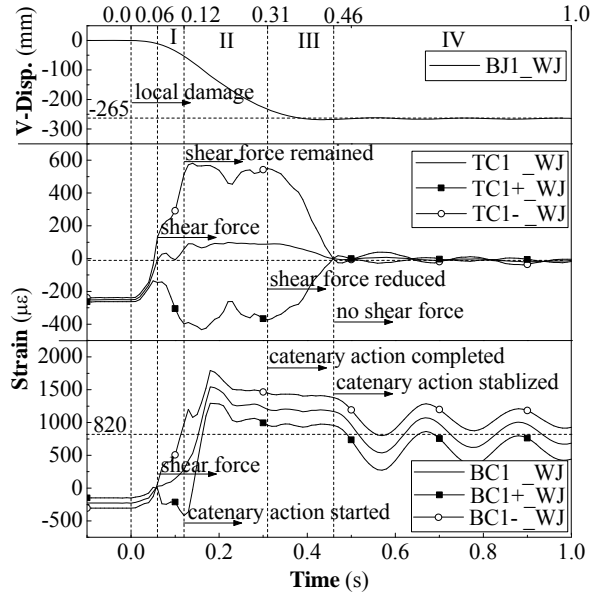
Fig. 11 Global internal force redistribution of truss-WJ

(a)

(b)
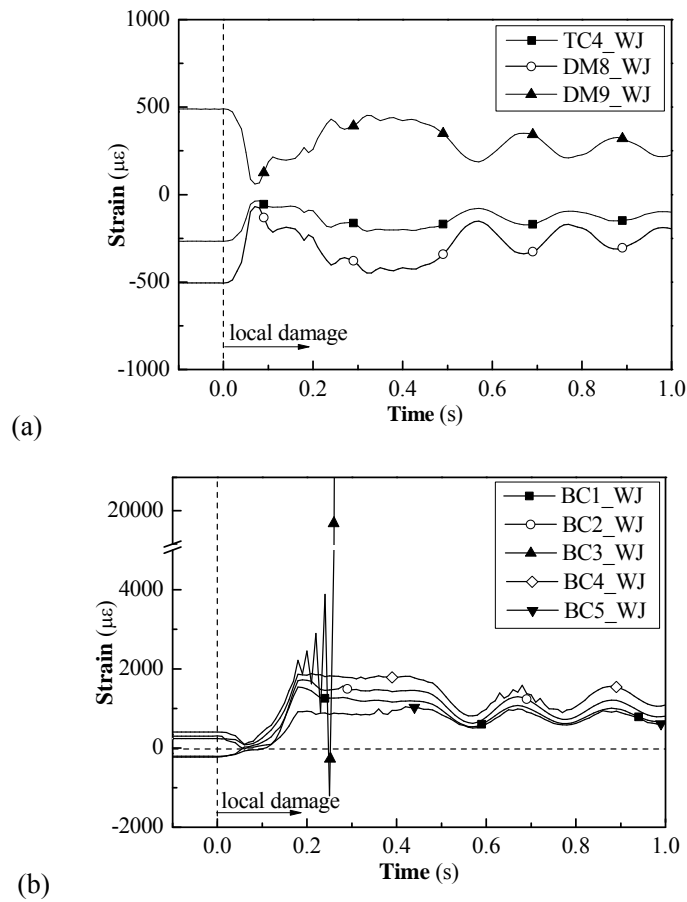
Fig. 12. Structural behavior of truss-WJ after local failure. (a) strain in TC4, DM8 and DM9; (b)

tensile strain in different bottom chords.

(a)

(b)

(c)

d)
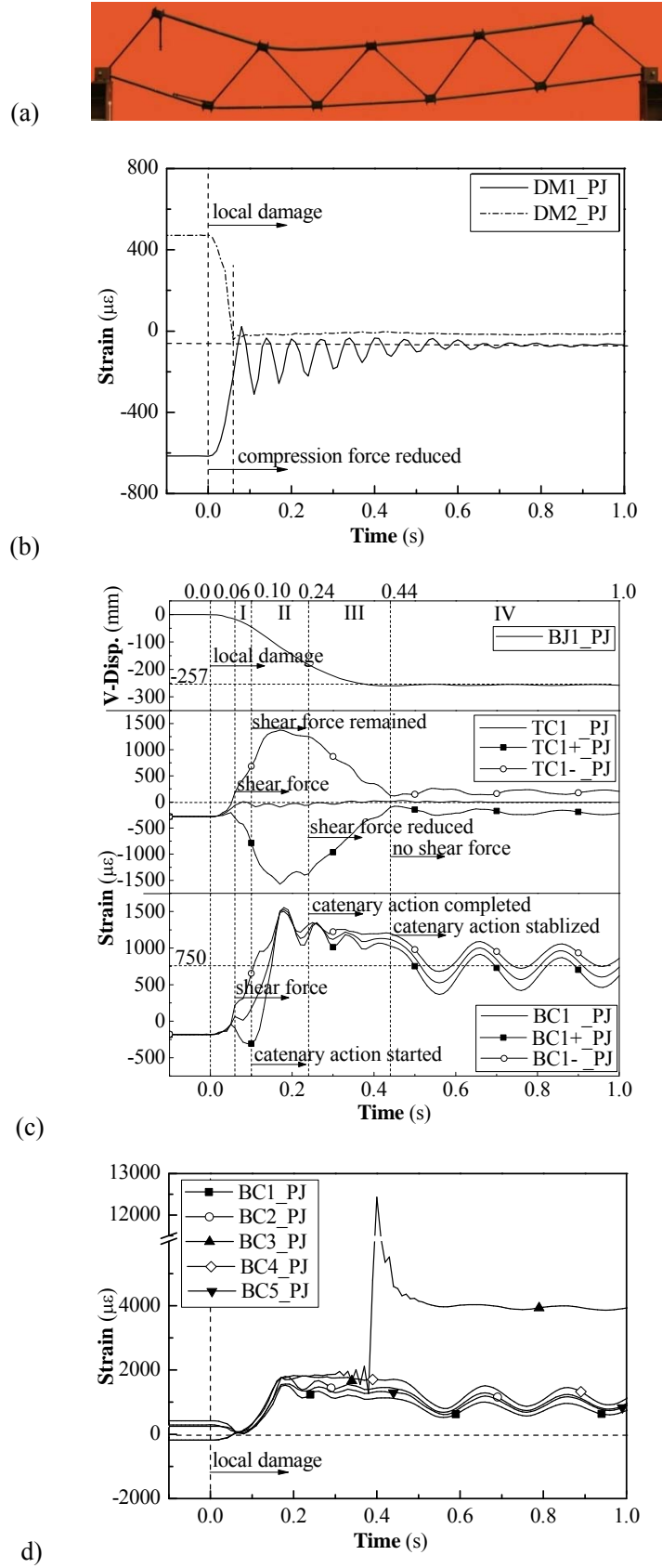
Fig. 13. Test results of truss-PJ. (a) balanced configuration; (b) local internal force redistribution

at TJ1; (c) global internal force redistribution; (d) tensile strain in different bottom chords.

Fig. 14. Truss-RJ collapsed due to the removal of DM2
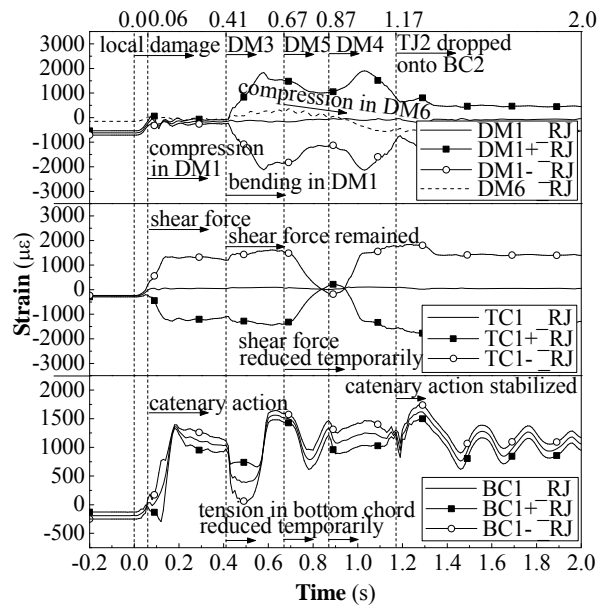
Fig. 15. Local and global internal force redistribution failed in truss-RJ due to the buckling of

diagonal members.
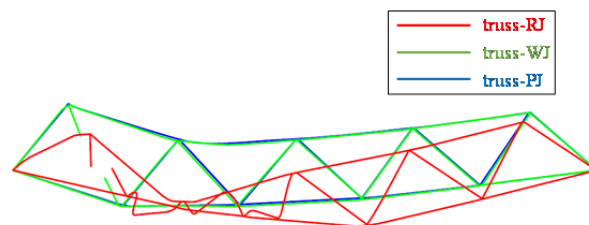
Fig. 16 Balanced configurations of the remaining structures of the three tested trusses.
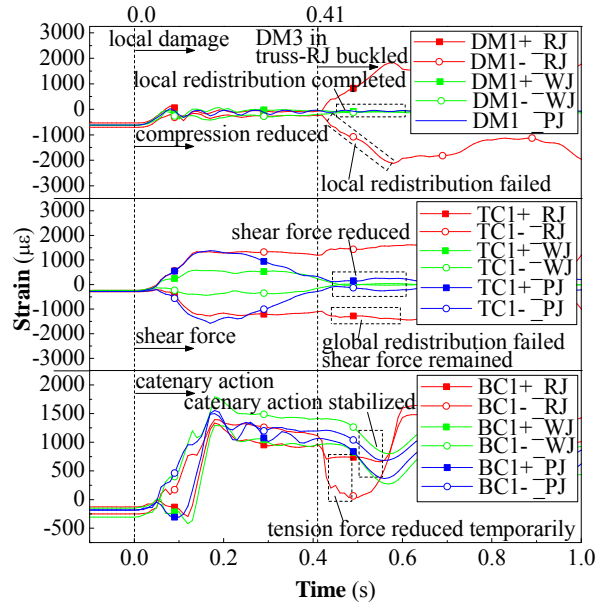
Fig. 17 Strain response of DM1, TC1 and BC1 in three tests
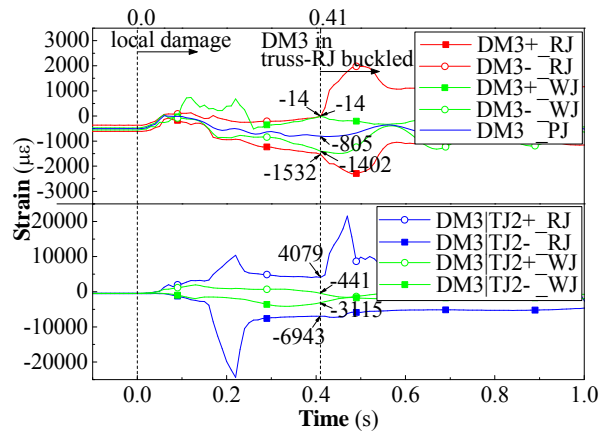
Fig. 18 Strain response of DM3 in three tests
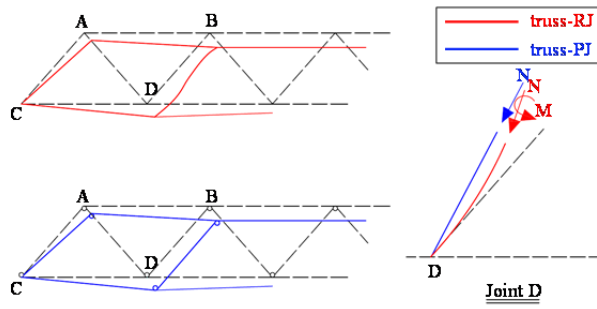
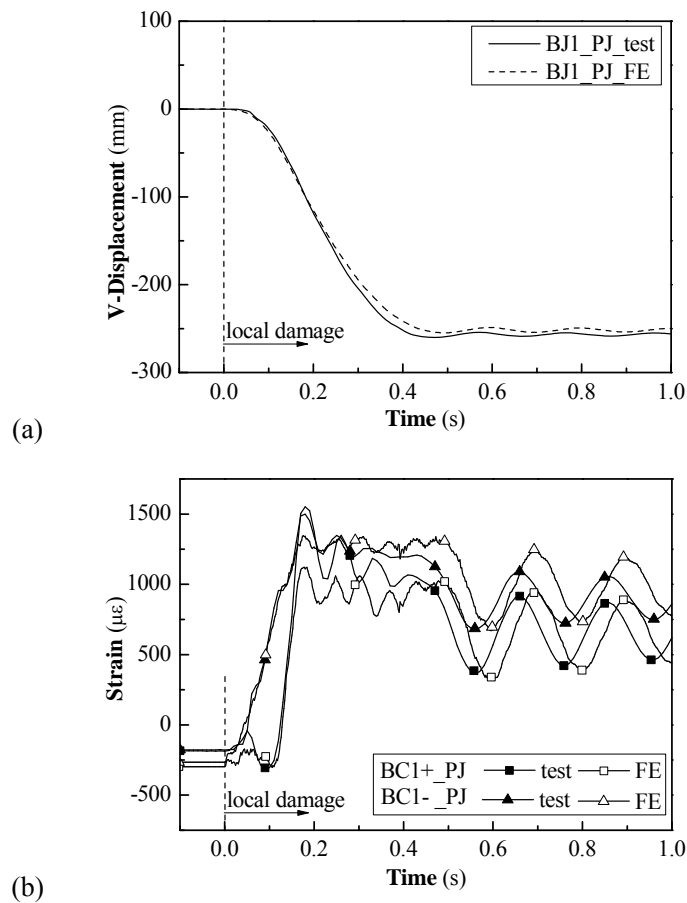Fig. 19 Bending moment is generated in truss with rigid joints when the catenary action

developed.

(a)

(b)

Fig. 20. Comparison of test and FE results of truss-PJ. (a) vertical displacement of BJ1; (b) strain
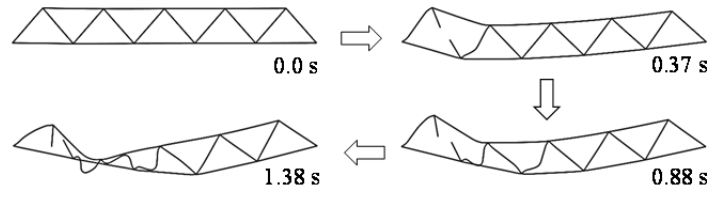responses in BC1.
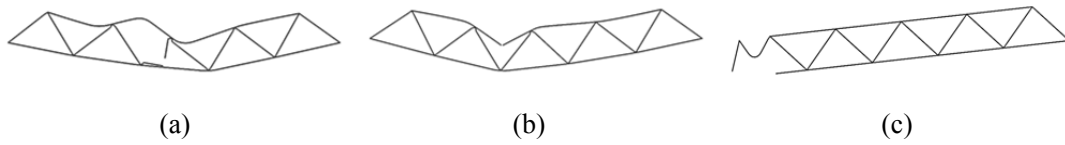
Fig. 21. Behavior of truss-RJ predicted by FE models.

| (a) | (b) | (c) |

Fig. 22 Behaviors of truss-PJ subjected to initial failure at different locations. (a) DM5; (b) TC2; (c) BC1.
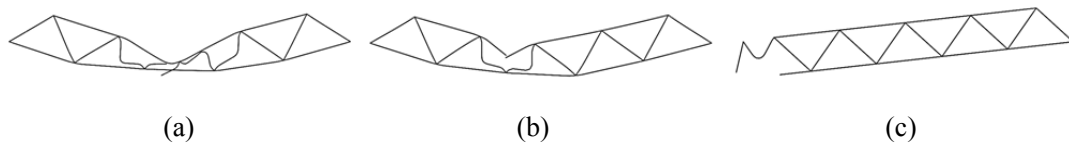

| (a) | (b) | (c) |

Fig. 23 Behaviors of truss-RJ subjected to initial failure at different locations. (a) DM5; (b) TC2; (c) BC1.